Performance Analysis of Transmitter-Side Cooperation–Receiver-Side-Relaying Schemes for Heterogeneous Sensor Networks

Azizollah Jamshidi, *Student Member, IEEE*, and Masoumeh Nasiri-Kenari, *Member, IEEE*

***Abstract*—In this paper, we present two physical layer cooperative protocols for heterogeneous sensor networks. There is one cooperator near the transmitter and a second cooperator (as a relay) near the receiver. Although the focus is on heterogeneous sensor networks, the methods can be applied to homogeneous sensor networks as well. Analytical and simulation results show that, under an additive white Gaussian noise channel assumption for the links between the transmitter and its partner and between the receiver and its partner, the proposed protocols achieve a diversity order of three or four by using the amplify-and-forward cooperation strategy and maximal ratio combining in the receiver. In addition, the proposed methods outperform the noncooperative single-hop transmission in the clustered heterogeneous sensor network and save a considerable amount of energy relative to the noncooperative transmission.**

***Index Terms*—Amplify-and-forward (AF) cooperation, cooperative diversity, heterogeneous sensor networks, maximal ratio combining.**

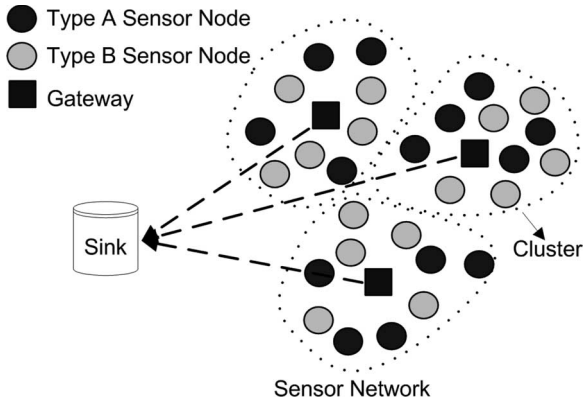

Fig. 1. Heterogeneous wireless sensor network with three types of sensor nodes.

I. Introduction

SENSOR networks are composed of a large number of nodes that sense certain phenomena in the area of interest and communicate their observations to other nodes or a central base station, such as a cluster head or a gateway for further processing. Due to the large number of sensing nodes and their computing and communication capabilities, many different applications for the home, military, habitat monitoring, and healthcare industry have become possible (for more details, see [1] and references therein).

Sensor networks are categorized as homogeneous and heterogeneous networks [2], [3]. In a homogeneous sensor network, the sensor nodes are identical in terms of computing, sensing and communication capabilities, and power supplies, whereas, in a heterogeneous sensor network, the nodes have different capabilities and/or power supplies [2]. In a homogeneous sensor network, data can be relayed using a multihop transmission or a cluster-based transmission. For example, in a data gathering application, multihop links are utilized to relay information to a sink, which is the ultimate destination of the data. In the cluster-based transmission, the cluster head gathers the information from the sensor nodes within its cluster via a single hop and then forwards the aggregated data directly to the sink or through the backbone of the cluster heads. In a heterogeneous network, first, some clusters are formed. In each cluster, a node that is rich in resources (high battery power, large memory, etc.) is deployed as a cluster head. Then, the cluster head collects data from the sensor nodes within its cluster, processes the data, and relays them toward the sink. Sensor nodes, which operate at low power and with limited memory, are used to collect data from the sensing field. In this paper, cluster heads are called gateways. Fig. 1 shows a clustered heterogeneous sensor network.

A critical aspect in the design of both homogeneous and heterogeneous wireless sensor networks is to save energy to extend the lifetime of the network. There are several energy saving mechanisms that can be used at different layers of a sensor network (for instance, see [10]–[19] and [29]).

Recently, cooperative communication has emerged as a promising physical layer scheme to design energy-efficient, high-throughput, and reliable physical links for wireless networks. The basic idea is that users or nodes in a wireless network share their information and cooperatively transmit as a virtual antenna array. Thus, diversity is achieved without requiring additional antennas at each node [20], [21]. Some repetition-based cooperative diversity algorithms, such as amplify-and-forward (AF) and decode-and-forward, are developed to exploit spatial diversity for reducing the outage probability at the cost of decreasing spectral efficiency [10], [17]–[19], [22]. Nicholas Laneman and Wornell [23] proposed a distributed space-time-coded protocol and showed that this

Manuscript received July 20, 2006; revised May 23, 2007, August 22, 2007, and August 25, 2007. The review of this paper was coordinated by Dr. M. Valenti.

The authors are with the Wireless Research Laboratory, Department of Electrical Engineering, Sharif University of Technology, Tehran, Iran (e-mail: a_jamshidi@ee.sharif.edu; mnasiri@sharif.edu).

Digital Object Identifier 10.1109/TVT.2007.909299

protocol can achieve full spatial diversity in the number of cooperating users. A different framework called coded cooperation was proposed in [24]–[26], in which each user, instead of repeating the received bits, attempts to transmit incremental redundancy for its partner. In wireless sensor networks, the cooperative scheme enhances the transmit energy efficiency. However, due to the involvement of the cooperating sensor nodes, it can increase the circuit energy consumption as well. Cui *et al.* [11] proposed a distributed multiple-input–multiple-output (MIMO) cooperative system based on the Alamouti space-time code [27]. The results have indicated that, in some cases, the cooperative MIMO-based sensor networks might provide better energy optimization and smaller end-to-end delay. Like in [11], a virtual MIMO-based cooperative communication for energy-limited sensor networks was developed in [14]. Both in [11] and [14], the authors have assumed error-free links among the cooperating nodes. Therefore, in the cooperative phase, each node has its partner's data, and the users can encode the transmission sequence according to the Alamouti space-time code. By the error-free link assumption, Cui *et al.* [11] and Jayaweera [14] simply have applied the bit error probability analysis of the traditional MIMO system to evaluate the energy consumption of their proposed cooperative space-time (CST) schemes. Moreover, Jayaweera [14] has assumed that the destination (data gathering node) can support multiple antennas and has incorporated the training overhead required in any MIMO-based systems.

In this paper, we combine the heterogeneous concept and the AF cooperation protocol [10] and assume a maximal ratio combiner (MRC) in the receivers for energy-efficient physical layer design in the wireless sensor network. We consider a system with one partner that cooperates with the transmitter and a second partner that cooperates with the receiver. Unlike in [11] and [14], we do not assume error-free links between the cooperating nodes, and we take into account the link noise between cooperators in our analysis including the bit error probability and outage probability, as well as the energy consumption. Like in [11], we assume binary phase-shift keying (BPSK) and multiquadrature amplitude modulation (M-QAM), and we optimize the energy consumption over the constellation. In addition, we consider the sensing energy, aggregation (signal processing) energy, and the effect of path loss exponent in our analysis. We evaluate the diversity gains of the proposed protocols via the outage probability and bit error probability analysis, and then, we study the energy consumption of the sensor nodes in the network. Despite the noisy links between the cooperating nodes, we show that our proposed practical schemes can save tremendous energy in the wireless sensor network compared to the noncooperative scheme.

The remainder of this paper is organized as follows: Section II introduces the system model and the mathematical description for the cooperative and noncooperative schemes. Section III characterizes the outage probability, bit error probability, and diversity behavior of the proposed protocols. Section IV provides the energy consumption analysis. Section V presents some numerical results and comparisons, and finally, Section VI summarizes our concluding remarks.

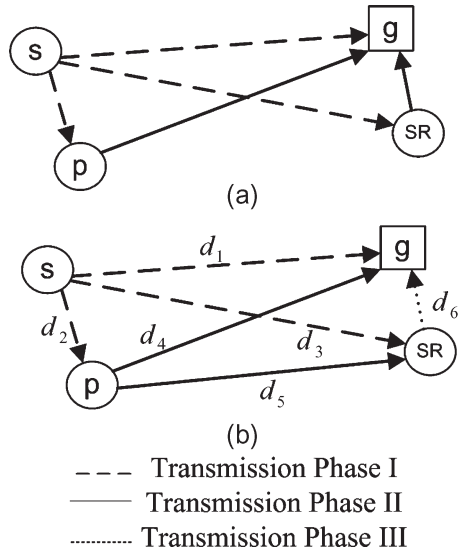

Fig. 2. Transmission phases. (a) Scheme one. (b) Scheme two.

II. System Model

Consider the heterogeneous sensor network of Fig. 1. We assume three types of sensor nodes with different functionalities in this network: type-A (gray) and type-B (black) nodes, which act as pure sensor nodes, and gateway nodes (square), which act as the cluster head nodes. The gateways can communicate directly or via a connected backbone among themselves. In addition, we assume that type-A nodes have fewer symbols than type-B nodes for transmission in the same time intervals, i.e., type-A nodes have smaller load than type-B nodes.[1] In the succeeding two sections, we describe our two proposed cooperative schemes and their mathematical descriptions.

A. Scheme One

1) Protocol Description: To illustrate the first cooperative scheme, consider the scenario depicted in Fig. 2(a), in which sensor nodes S and P (both of them have similar types, i.e., types A or B, and therefore, they have the same transmission loads) transmit to gateway G by using a type-A sensor node as a semirelay node (node SR) [Fig. 2(a) considers the transmission of node S to the gateway[2]]. In fact, node SR is a relay in the receiver side, and we assume that the semirelay (node SR) not only helps sensor nodes S and P but also sends its own few information symbols to the gateway.

The first cooperative scheme consists of two transmission phases [see Fig. 2(a)]. In the first phase, source node S transmits an information symbol to the partner, the semirelay, and the gateway nodes. Then, in the second phase, the semirelay and the partner amplify the received signals and send them to the gateway through two independent channels by using the AF cooperation protocol strategy. Now, the gateway combines

[1]Throughout this paper, we assume that all of the sensor nodes have the same battery energies.

[2]In Fig. 2(a), node P acts as a partner for node S and helps node S in transmission toward the SR and gateway nodes. However, because of the symmetry, node S can also act as a partner for node P and help it in the transmission toward the SR and gateway nodes.

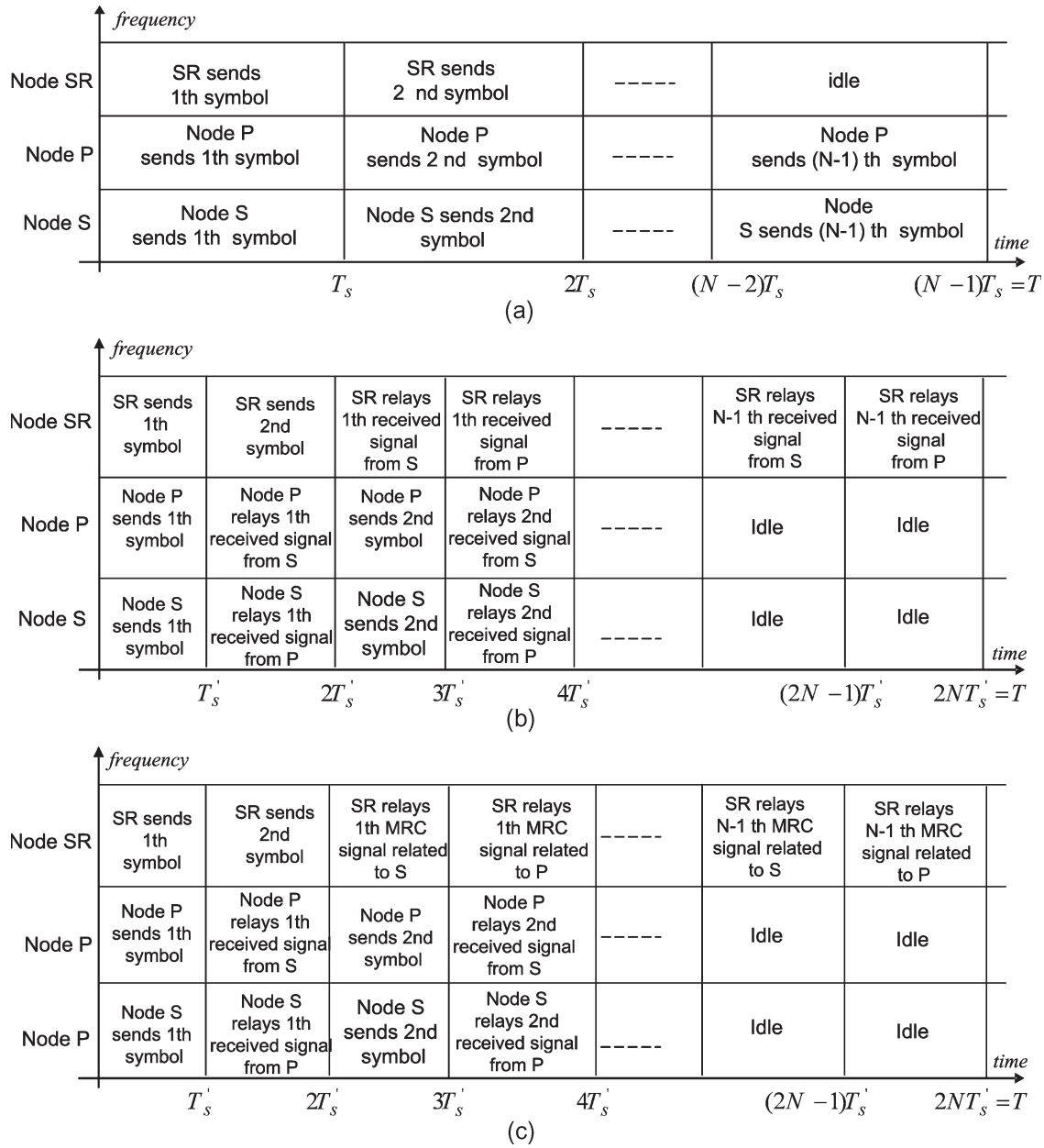

Fig. 3. Orthogonal channel assignment. (a) Noncooperative scheme. (b) Scheme one. (c) Scheme two.

these independent received signals with the MRC rule and makes a decision about the transmitted symbol. We expect this scheme to achieve a diversity order of three. To prevent interference, several efficient medium-access-control layer schemes have been proposed for wireless sensor networks, such as fixed allocation, scheduled time-division multiple access (TDMA) [33], and random-access versions [1]. For the sake of simplicity, we consider the frequency-division multiple access/TDMA [34] orthogonal channel assignments of Fig. 3(a) and (b) for the noncooperative and cooperative schemes, respectively. We assume that each transmission block has a duration of T seconds. In the noncooperative scheme, nodes P and S independently transmit blocks of length $(N-1)$ symbols in two orthogonal channels. However, node SR sends only two symbols in another orthogonal channel and remains idle in the remaining $(N-3)$ symbol intervals of the block (low-load node) [see Fig. 3(a)]. The time schedule of the first cooperative scheme is depicted in Fig. 3(b). As is clear from Fig. 3(b), to maintain the same effective symbol transmission rate as the noncooperative scheme, each block interval of length T contains $2N$ symbol intervals in this cooperative scheme. Nodes S and P transmit $(2N-2)$ symbols in each block and remain idle in the last two symbol intervals. In addition, node SR sends its own two information symbols and the $2N-2$ received symbols of nodes S and P in $2N$ symbol intervals of its block according to Fig. 3(b).

2) Mathematical Description: We assume that the links between nodes S and P and between node SR and the gateway can be modeled as additive white Gaussian noise (AWGN) channels, and the other links (Fig. 2) are modeled as flat Rayleigh fading channels. Due to the symmetry of the channel allocations, we only focus on the data transmission of node S. Node S employs nodes P and SR as relays; therefore, the

first phase of transmission can be mathematically described as follows [see the time schedule presented in Fig. 3(b)]:

$$y_{P,S}[i] = \sqrt{\varepsilon} x_S[i] + z_{P,S}[i] \quad i = 1, 3, 5, \ldots, 2N-3 \tag{1}$$

$$y_{\mathrm{SR},S}[i] = \sqrt{\varepsilon'} a_{\mathrm{SR},S} x_s[i] + z_{\mathrm{SR},S}[i] \quad i = 1, 3, 5, \ldots, 2N-3 \tag{2}$$

$$y_{G,S}[i] = \sqrt{\varepsilon'} a_{G,S} x_S[i] + z_{G,S}[i] \quad i = 1, 3, 5, \ldots, 2N-3 \tag{3}$$

where $x_S[i]$ is the source transmitted signal, and $y_{P,S}[i]$, $y_{\mathrm{SR},S}[i]$, and $y_{G,S}[i]$ are the partner, the semirelay, and the gateway received signals from node S, respectively. ε is the average energies of the received signals (excluding the noise term) in node SR and the gateway when they receive the signals from either node S or node P, and ε' is the average energy of the received signal (excluding the noise term) in node P from node S or in the gateway from node SR.[3] We assume that the information-bearing symbols $x_S[i]$'s are drawn from a constellation with unit average energy, i.e., $E\{|x_S[i]|^2\} = 1$, where $E\{.\}$ stands for the expectation. $a_{k,j}$ indicates the channel random gain between the jth transmitter and the kth receiver, and $z_{k,j}[i]$ represents the noise component in the kth receiver during the ith signaling interval. The noise terms are modeled as independent zero-mean symmetrical complex Gaussian random variables with a variance of $N_o/2$ for each dimension; in addition, fading coefficients $a_{k,j}$'s are modeled as independent symmetrical complex Gaussian-distributed random variables with zero mean and a variance of 1/2 for each dimension.[4] For a slow flat fading channel, the fading coefficients remain constant over each transmission block, i.e., we assume constant fading coefficients over each block of $2N$ information symbols.

For the second phase of transmission, both nodes P and SR send an amplified version of the received signals to the gateway. Note that node SR ignores the received signal from node P during the second phase of transmission. In this phase, from Fig. 3(b), we have

$$y_{G,P}[i] = \beta a_{G,P} y_{P,S}[i-1] + z_{G,P}[i] \quad i = 2, 4, \ldots, 2N-2 \tag{4}$$

$$y_{G,\mathrm{SR}}[i] = \beta' y_{\mathrm{SR},S}[i-2] + z_{G,\mathrm{SR}}[i] \quad i = 3, 6, \ldots, 2N-3 \tag{5}$$

where $y_{G,P}[i]$ and $y_{G,\mathrm{SR}}[i]$ are the gateway received signals via nodes P and SR, respectively. $a_{G,P}$, $z_{G,P}[i]$, and $z_{G,\mathrm{SR}}[i]$ are defined as $a_{k,j}$ and $z_{k,j}[i]$ in (1)–(3). In addition, to remain within their received energy constraints, the average energies of the received signals (excluding the noise term) at node G from nodes P and SR must be equal to ε' and ε, respectively. As a result, nodes P and SR must set their amplification gains, i.e., β and β', which are given in (4) and (5), respectively, such that [10]

$$E\left\{|\beta a_{G,P} y_{P,S}|^2\right\} = E\left\{|\beta y_{P,S}|^2\right\} = \varepsilon'$$
$$E\left\{|\beta' y_{\mathrm{SR},S}|^2\right\} = \varepsilon. \tag{6}$$

Therefore

$$\beta = \sqrt{\frac{\varepsilon'}{\varepsilon + N_o}}$$
$$\beta' = \sqrt{\frac{\varepsilon}{\varepsilon' + N_o}}. \tag{7}$$

Note that, in the first equation of (6), the second equality comes from the fact that $a_{G,P}$ and $y_{P,S}$ are independent and that $E\{|a_{G,P}|^2\} = 1$.

B. Scheme Two

1) Protocol Description: Consider the channel assignment of Fig. 3(c) and the scenario depicted in Fig. 2(b). In the sensor networks, we are interested in the scenario where d_2 and d_6 are considerably smaller than d_1, d_3, d_4, and d_5, as depicted in Fig. 2(b). This allows reliable communication between nodes S and P or between the semirelay and the gateway. Therefore, this scenario is similar to a MIMO system with two transmitter and two receiver antennas. Therefore, we can construct another scheme called "scheme two," which can achieve a diversity order of four. Scheme two has three phases of transmission [see Fig. 2(b)]. In the first phase, like in scheme one, node S transmits its information symbol to node P, node SR, and the gateway. Then, in the second phase, node P amplifies and sends its received signal to node SR and the gateway through two independent channels. In the third phase, the semirelay node combines two independent received signals in the last two phases of transmissions by using the MRC technique. Finally, the semirelay node amplifies and transmits the combined signal to the gateway. The gateway uses these three signals received in three phases in a proper manner to decide about the transmitted symbol.

2) Mathematical Description: Because of the similarity between schemes one and two in the first phase of transmission, we can use the descriptions in (1)–(3) for scheme two as well. However, in the second phase of transmission, both the gateway and node SR consider the received signal from node P. Therefore, from Fig. 3(c), the received signals from node P are

$$y_{G,P}[i] = \beta a_{G,P} y_{P,S}[i-1] + z_{G,P}[i] \quad i = 2, 4, \ldots, 2N-2 \tag{8}$$

$$y_{\mathrm{SR},P}[i] = \beta a_{\mathrm{SR},P} y_{P,S}[i-1] + z_{\mathrm{SR},P}[i] \quad i = 2, 4, \ldots, 2N-2 \tag{9}$$

where β is given in (7). In the last transmission phase of scheme two, first, node SR combines the received signals in the first and second phases of transmission, which are given in (2)

[3]Because of the proximities of node S to node P and of the semirelay to the gateway, distances d_1, d_3, d_4, and d_5 in Fig. 2(b) are nearly equal; therefore, the received energies in (2) and (3) are equal.

[4]Note that ε and ε' capture the path loss effects, and as a result, we normalize the complex fading coefficient variance to 1.

and (9), respectively, by using the MRC technique; therefore, we have

$$x_{\mathrm{MRC}}[i] = \frac{\beta\sqrt{\varepsilon}a^*_{\mathrm{SR},P}}{\beta^2|a_{\mathrm{SR},P}|^2N_o + N_o}y_{\mathrm{SR},P}[i-1] + \frac{\sqrt{\varepsilon'}a^*_{\mathrm{SR},S}}{N_o}y_{\mathrm{SR},S}[i-2], \qquad i = 3, 6, \ldots, 2N-3 \tag{10}$$

where x_{MRC} is the combined signal in node SR, and $*$ denotes the complex conjugate. After amplifying, node SR then transmits the preceding combined signal to the gateway by using the AF strategy. Thus, the gateway receives the following signal:

$$y_{G,\mathrm{SR}}[i] = \beta'' x_{\mathrm{MRC}}[i] + z_{G,\mathrm{SR}}[i], \qquad i = 3, 6, \ldots, 2N-3. \tag{11}$$

Because of the similarity between two Gaussian links (the link between nodes S and P and the link between node SR and the gateway), we assume that the average received energy at the gateway from node SR is the same as the average received energy at node P from node S in the first phase of transmission. Therefore, node SR must use an amplification gain β'' such that

$$E\left\{|\beta'' x_{\mathrm{MRC}}|^2\right\} = \varepsilon. \tag{12}$$

To compute the value β'', first, we expand (9) by using (1). Then, by substituting (2) and (9) in (10) and applying some algebraic manipulation, we easily obtain

$$\beta'' = \sqrt{\frac{\varepsilon}{\mathrm{SNR}^2_{\mathrm{SR}} + \mathrm{SNR}_{\mathrm{SR}}}} \tag{13}$$

where $\mathrm{SNR}_{\mathrm{SR}}$ is given by

$$\begin{aligned}\mathrm{SNR}_{\mathrm{SR}} &= \frac{|a_{\mathrm{SR},S}|^2\varepsilon'}{N_o} + \frac{\beta^2\varepsilon|a_{\mathrm{SR},S}|^2}{\beta^2|a_{\mathrm{SR},P}|^2N_o + N_o} \\ &= \eta_{\mathrm{SR},S} + \frac{\eta_{\mathrm{SR},P}\eta_{P,S}}{\eta_{\mathrm{SR},P} + \eta_{P,S} + 1} \\ &\simeq \eta_{\mathrm{SR},S} + \eta_{\mathrm{SR},P}.\end{aligned} \tag{14}$$

$\eta_{i,j}$ denotes the instantaneous received signal-to-noise ratio (SNR) and is defined as follows:

$$\begin{aligned}\eta_{i,j} &= \frac{\varepsilon'|a_{i,j}|^2}{N_o}, \qquad i \in \{G, \mathrm{SR}\}; \quad j \in \{S, P\} \\ \eta_{P,S} &= \eta_{G,\mathrm{SR}} = \frac{\varepsilon}{N_o}.\end{aligned} \tag{15}$$

As stated in the previous section, we assume that d_2 and d_6 are much smaller than d_1, d_3, d_4, and d_5. On the other hand, we know that $(\varepsilon/\varepsilon') = \kappa(d_1/d_2)^\alpha$ for some constant κ, where α is the path loss exponent, which is equal to 2 for free space and is greater than 2 for more scattering environments. As a result, ε is much greater than ε'. By this assumption, the approximation in (14) holds.

III. Outage and Bit Error Probabilities

In this section, we derive the outage probability P_{out} and bit error probability P_b of the proposed schemes. For P_b derivation, we consider a system with BPSK modulation or M-QAM modulation with a constellation size of $M = 2^b$ (b bit/symbol) and a coherent receiver. In addition, we suppose that the receivers, and not the transmitters, know the fading coefficients via training pilot sequences. We consider the probability of outage as a performance criterion [10], [20]. As a function of the fading coefficients, the mutual information for each scheme is a random variable denoted by I. Thus, for target rate R, the outage probability denoted by P_{out} is the probability that $I < R$.

A. First Scheme Analysis

As stated in Section II-A, considering the transmitted signal by node S as an input and the received signals in the gateway as outputs, scheme one produces equivalent one-input, three-output complex Gaussian noise channels with different attenuations and noise levels. In Appendix A, we show that the maximum mutual information between node S and the gateway, which is achieved by an independent identically distributed (i.i.d.) Gaussian input, is

$$I_1 = \frac{(N-1)}{2N}\log_2\left(1 + \eta_{G,S} + \frac{\eta_{P,S}\eta_{G,P}}{\eta_{P,S} + \eta_{G,P} + 1} + \frac{\eta_{\mathrm{SR},S}\eta_{G,\mathrm{SR}}}{\eta_{\mathrm{SR},S} + \eta_{G,\mathrm{SR}} + 1}\right) \tag{16}$$

where the $\eta_{i,j}$'s are defined in (15). With the zero-mean mutually independent complex Gaussian-distributed fading coefficients with a variance of 1, we readily find that $\eta_{G,S}$, $\eta_{G,P}$, and $\eta_{\mathrm{SR},S}$ are i.i.d. exponential random variables with a mean equal to Λ. Λ is easily computed as follows:

$$\Lambda = \frac{\varepsilon'}{N_o}. \tag{17}$$

Note that Λ also indicates the average received SNR. As previously stated in deriving (14) and (15), with the assumption of $d_1 \gg d_2$, ε is much greater than ε', and as a result, $\eta_{G,P}$ and $\eta_{\mathrm{SR},S}$ are substantially smaller than $\eta_{P,S}$ and $\eta_{G,\mathrm{SR}}$. Therefore, in (16), by neglecting the terms $\eta_{G,P} + 1$ and $\eta_{\mathrm{SR},S} + 1$ against $\eta_{P,S}$ and $\eta_{G,\mathrm{SR}}$, we easily obtain

$$I_1 \simeq \frac{N-1}{2N}\log_2(1 + \eta_{G,S} + \eta_{G,P} + \eta_{\mathrm{SR},S}). \tag{18}$$

The preceding result shows that scheme one is equal to a one-input, three-output communication system with three identical and independent Rayleigh fading channels. Our simulation results will verify that (18) is a good approximation[5] of (16).

[5]It can be easily shown that (18) is also an upper bound for the mutual information of scheme one.

Thus, from (18), the approximated outage probability for scheme one can be computed as (see Appendix B)

$$P_{\text{out}}^1 = \Pr(I_1 < R) \simeq \gamma_{\text{inc}}\left(3, \frac{2^{\left(\frac{2N}{N-1}\right)R} - 1}{\Lambda}\right) \tag{19}$$

where γ_{inc} is an incomplete gamma function [30, pp. 40]. Now, we consider the high-SNR and fixed-rate regimes. In Appendix B, we show that the asymptotic behavior of P_{out}^1 is given by

$$P_{\text{out}}^1 \sim \frac{1}{6}\left(\frac{2^{\left(\frac{2N}{N-1}\right)R} - 1}{\Lambda}\right)^3 \text{ for a large } \Lambda. \tag{20}$$

Note that, in the preceding equation, for continuous functions f and g, the relation "$f(\Lambda) \sim g(\Lambda)$" means that $\lim_{\Lambda\to\infty} f(\Lambda)/g(\Lambda) = 1$. As the preceding result indicates, for fixed-rate and high-SNR regimes, scheme one achieves third-order diversity.

For scheme one, we can identify three independent receiving paths in the gateway. As a result, by using BPSK modulation (1 b/symbol) and a coherent MRC receiver in the gateway, the bit error probability conditioned on the instantaneous SNR is given by [28]

$$\begin{aligned} P^1_{b|\eta_{G,S},\eta_{G,P},\eta_{\text{SR},S}} &= Q(\sqrt{2\text{SNR}}) \\ &= Q\left(\sqrt{2\left(\eta_{G,S} + \frac{\eta_{P,S}\eta_{G,P}}{\eta_{P,S}+\eta_{G,P}+1} + \frac{\eta_{\text{SR},S}\eta_{G,\text{SR}}}{\eta_{\text{SR},S}+\eta_{G,\text{SR}}+1}\right)}\right) \\ &\simeq Q\left(\sqrt{2(\eta_{G,S}+\eta_{G,P}+\eta_{\text{SR},S})}\right) \end{aligned} \tag{21}$$

where SNR is the total instantaneous received SNR via the three independent paths, and the $\eta_{i,j}$'s are defined in (15). Moreover, for M-QAM with a square constellation (even b), the conditional symbol error probability is given by [32]

$$\begin{aligned} P^1_{s|\eta_{G,S},\eta_{G,P},\eta_{\text{SR},S}} &= 4\left(1 - \frac{1}{\sqrt{M}}\right) Q\left(\sqrt{\frac{3\text{SNR}}{M-1}}\right) \\ &\quad - 4\left(1 - \frac{1}{\sqrt{M}}\right)^2 Q^2\left(\sqrt{\frac{3\text{SNR}}{M-1}}\right) \text{ for } b \geq 2 \end{aligned} \tag{22}$$

where SNR is defined in (21), and $M = 2^b$ is the number of constellation symbols. When b is odd, we may still use (22) as a tight upper bound for the symbol error probability after dropping the terms $(1 - (1/\sqrt{M}))$ and $(1 - (1/\sqrt{M}))^2$. By averaging on fading coefficients, the unconditioned bit error probability for BPSK and M-QAM is derived as [32]

$$\begin{aligned} P_b^1 = &\left(\frac{1 - \sqrt{\frac{\Lambda}{1+\Lambda}}}{2}\right)^L \sum_{l=0}^{L-1} \binom{L-1+l}{l} \\ &\times \left(\frac{1 + \sqrt{\frac{\Lambda}{1+\Lambda}}}{2}\right)^l \text{ for BPSK} \end{aligned} \tag{23}$$

and

$$\begin{aligned} P_b^1 \simeq &\frac{4}{b}\left(1 - \frac{1}{\sqrt{M}}\right)\left(\frac{1-\mu_c}{2}\right)^L \sum_{l=0}^{L-1}\binom{L-1+l}{l} \\ &\times \left(\frac{1+\mu_c}{2}\right)^l - 4\left(1 - \frac{1}{\sqrt{M}}\right)^2 \\ &\times \left(\frac{1}{4} - \frac{\mu_c}{\pi}\left(\left[\frac{\pi}{2} - \tan^{-1}\mu_c\right]\sum_{l=0}^{L-1}\frac{(2l\,l)}{[4(1+g\Lambda)]^l}\right.\right. \\ &- \sin(\tan^{-1}\mu_c)\sum_{l=1}^{L-1}\sum_{i=1}^{l}\frac{T_{il}}{(1+g\Lambda)^l} \\ &\left.\left.\times\left[\cos(\tan^{-1}\mu_c)\right]^{2(l-i)+1}\right)\right) \end{aligned} \tag{24}$$

for M-QAM, where Λ is given by (17), L is three (in this three-path scheme), and $g = 3/[2(M-1)]$. In addition, T_{il} and μ_c are defined as follows:

$$T_{il} = \frac{\binom{2l}{l}}{\binom{2(l-i)}{l-i}4^i\,(2(l-i)+1)}$$

$$\mu_c = \sqrt{\frac{g\Lambda}{1+g\Lambda}}.$$

In (24), we have used the formula of the bit error probability for M-QAM with square constellations (b is an even number) to approximate probability P_b^1 for all values of $b \geq 2$. The introduced error when b is odd is negligible for our purposes. We utilize these results in the energy consumption analysis in Section IV.

B. Second Scheme Analysis

We begin with (10), and from (2) and (9), we obtain

$$\begin{aligned} x_{\text{MRC}}[i+2] = &\left(\frac{|a_{\text{SR},S}|^2\varepsilon'}{N_o} + \frac{\beta^2\varepsilon|a_{\text{SR},P}|^2}{\beta^2|a_{\text{SR},P}|^2N_o + N_o}\right)x_S[i] \\ &+ \frac{\sqrt{\varepsilon'}a^*_{\text{SR},S}}{N_o}z_{\text{SR},S}[i] + \frac{\beta\sqrt{\varepsilon}a^*_{\text{SR},P}}{\beta^2|a_{\text{SR},P}|^2N_o + N_o} \\ &\times\left(\beta a_{\text{SR},P}z_{P,S}[i] + z_{\text{SR},P}[i+1]\right), \\ &i = 1, 2, \ldots, 2N-3. \end{aligned} \tag{25}$$

The total noise term in the preceding equation has a complex Gaussian distribution with zero mean and variance equal to $\mathrm{SNR}_{\mathrm{SR}}$, where $\mathrm{SNR}_{\mathrm{SR}}$ is given by (14). Now, the gateway combines the signals received from the source, partner, and semirelay, which are given by (3), (8), and (11), respectively, to obtain a proper statistics for the optimum detection. By substituting (1) in (8) and comparing the result with (25), we observe that, because of the common noise term $z_{P,S}[i]$, the signals received from the partner and the semirelay at the gateway are dependent, and as a result, the MRC is not an optimum receiver for the gateway. In Appendix C, we show that the optimum detector has the following complicated decision rule for the BPSK modulation:

$$Z = (2Db_1 y_{G,S} + (2Eb_2 + Gb_3) y_{G,P} + (2Fb_3 + Hb_2) y_{G,\mathrm{SR}} \underset{+1}{\overset{-1}{\gtrless}} 0 \quad (26)$$

where coefficients D, E, F, H, b_1, b_2, and b_3 are some constants that are defined in (67)–(70), which are shown in Appendix C. The inequality relationship "$\underset{+1}{\overset{-1}{\gtrless}}$" indicates that the transmitted symbol is -1 (bit 0) if decision variable Z is positive; otherwise, it is $+1$ (bit 1). The preceding decision rule is complicated and renders an analysis of the proposed protocol feasible only through computer simulations. Fortunately, for the considered scenario, ε is greater than ε'; therefore, parameter β defined in (7) is much smaller than one. As a result, we can neglect the noise term $\beta a_{\mathrm{SR},P} z_{P,S}[i]$ in (25) against the other noise terms and approximate (25) as follows:

$$\tilde{x}_{\mathrm{MRC}}[i+2] = \left(\frac{|a_{\mathrm{SR},P}|^2 \varepsilon'}{N_o} + \frac{\beta^2 \varepsilon |a_{\mathrm{SR},P}|^2}{\beta^2 |a_{\mathrm{SR},P}|^2 N_o + N_o} \right) x_S[i] + \frac{\sqrt{\varepsilon'} a^*_{\mathrm{SR},S}}{N_o} z_{\mathrm{SR},S}[i] + \frac{\beta \sqrt{\varepsilon} a^*_{\mathrm{SR},P}}{\beta^2 |a_{\mathrm{SR},P}|^2 N_o + N_o} z_{\mathrm{SR},P}[i+1] \quad i = 1, 2, \ldots, 2N-3. \quad (27)$$

Now, with the preceding approximation, by substituting (27) in (11), from (3), (8), and (11), three signals received from the source, partner, and semirelay will be independent; therefore, the optimum detector reduces to the MRC detector. It is well known that, conditioned on the fading coefficients, the total instantaneous SNR for the MRC detector is given as follows:

$$\mathrm{SNR}_T = snr_1 + snr_2 + snr_3 \quad (28)$$

where snr_i is the instantaneous received SNR via the ith independent path. By using (3) for path 1 (received signal through node S), (8) for path 2 (received signal through node P), and (11) [in which x_{MRC} is substituted with the approximated semirelay combined signal $\tilde{x}_{\mathrm{MRC}}$ given in (27)] for path 3, the snr_i's are computed as

$$\begin{aligned} snr_1 &= \frac{|a_{G,S}|^2 \varepsilon'}{N_o} = \eta_{G,S} \\ snr_2 &= \frac{\beta^2 \varepsilon |a_{G,P}|^2}{(\beta^2 |a_{G,P}|^2 + 1) N_o} = \frac{\eta_{P,S} \eta_{G,P}}{\eta_{P,S} + \eta_{G,P} + 1} \\ snr_3 &= \frac{\beta''^2 \mathrm{SNR}^2_{\mathrm{SR}}}{N_o (1 + k_3^2 + k_5^2)} \end{aligned} \quad (29)$$

where k_3 and k_5 are defined in (63). By substituting the values of β and β'', which are given in (7) and (13), into k_3 and k_5, respectively, and after some straightforward simplifications, we obtain

$$snr_3 = \frac{\mathrm{SNR}^2_{\mathrm{SR}}}{\frac{1}{\eta_{P,S}} \left(\mathrm{SNR}_{\mathrm{SR}} + \mathrm{SNR}^2_{\mathrm{SR}} \right) + \eta_{\mathrm{SR},S} + \frac{\eta_{P,S} \eta_{\mathrm{SR},P} (\eta_{P,S}+1)}{(\eta_{P,S} + \eta_{\mathrm{SR},P} + 1)^2}} \quad (30)$$

where $\mathrm{SNR}_{\mathrm{SR}}$ and its approximated value are given in (14). Now, if we consider that the Gaussian links are stronger than the Rayleigh links, we can apply some approximations that are similar to the one used in (14), and consequently, we can approximate snr_2 and snr_3 in (29) and (30) as (31), shown at the bottom of the page. In (31), the last approximation is due to the fact that, in sufficiently strong Gaussian links, we can assume $\eta_{P,S} \gg \eta_{\mathrm{SR},S} + \eta_{\mathrm{SR},P}$. Therefore, from (29)–(31), (28) can be approximated as

$$\mathrm{SNR}_T = \eta_{G,S} + \eta_{G,P} + \eta_{\mathrm{SR},S} + \eta_{\mathrm{SR},P} \quad (32)$$

which is, in fact, equal to the result for a well-known diversity path combining over four independent Rayleigh fading channels; thus, the unconditional bit error probabilities for the BPSK and M-QAM modulations, i.e., P_b^2, are given by (23) and (24), respectively, with $L = 4$.

$$\begin{aligned} snr_2 &\simeq \eta_{G,P} \\ snr_3 &\simeq \frac{(\eta_{\mathrm{SR},S} + \eta_{\mathrm{SR},P})^2}{\frac{1}{\eta_{P,S}} (\eta_{\mathrm{SR},S} + \eta_{\mathrm{SR},P} + (\eta_{\mathrm{SR},S} + \eta_{\mathrm{SR},P})^2) + \eta_{\mathrm{SR},S} + \frac{(1+\eta_{P,S}) \eta_{\mathrm{SR},P}}{\eta_{P,S} + \eta_{\mathrm{SR},P} + 1}} \\ &\simeq \frac{\eta_{P,S} (\eta_{\mathrm{SR},S} + \eta_{\mathrm{SR},P})}{\eta_{\mathrm{SR},S} + \eta_{\mathrm{SR},P} + \eta_{P,S}} \simeq \eta_{\mathrm{SR},S} + \eta_{\mathrm{SR},P} \end{aligned} \quad (31)$$

The numerical results given in Section V will show that the MRC detector is a good approximation for the optimum detector (see Fig. 5). Therefore, neglecting the noise term $\beta a_{\mathrm{SR},P} z_{P,S}[i]$ in (25) at the gateway has a negligible effect on the performance of the proposed scheme two in the considered scenario. For the outage probability analysis, we neglect this noise term and derive the mutual information and, consequently, the outage probability based on the preceding approximation. In Appendix C, we show that the mutual information between the source and the gateway by neglecting the noise term is

$$I(x_S, y_2) \simeq \frac{N-1}{2N} \log_2(1 + snr_1 + snr_2 + snr_3) \quad (33)$$

where the snr_i's are defined in (29). By using the approximated values for snr_2 and snr_3 given in (31), we obtain

$$I(x_S, y_2) \simeq \frac{(N-1)}{2N} \log_2(1 + \eta_{G,S} + \eta_{G,P} + \eta_{\mathrm{SR},S} + \eta_{\mathrm{SR},P}). \quad (34)$$

Note that, exactly like the procedures taken in Appendix B to derive P_{out}^1 from the mutual information, we can derive the outage probability based on the approximation given in (34) as follows:

$$P_{\mathrm{out}}^2 \simeq \gamma_{\mathrm{inc}} \left(4, \frac{2^{\left(\frac{2N}{N-1}\right)R} - 1}{\Lambda} \right) \quad (35)$$

where Λ is defined in (17), and R is the target rates of the cooperating nodes S and P.

At the high-SNR and fixed-rate regimes, the asymptotic behavior of $P_{\mathrm{out}}^2$is given as follows:

$$P_{\mathrm{out}}^2 \sim \frac{1}{24} \left(\frac{2^{\left(\frac{2N}{N-1}\right)R} - 1}{\Lambda} \right)^4. \quad (36)$$

From (36), we conclude that scheme two achieves a fourth-order diversity.

IV. Energy Consumption Analysis

We consider a general communication link connecting two wireless nodes. To consider the energy consumption for the transmission of one message bit, energy consumption in all blocks of the transmitter and the receiver has to be considered. Usually, the energy consumption of a sensor node is due to sensing, computation (aggregation), and communication components [31]. Like in [31], we assume that the energy required to sense a bit is a constant denoted by $\varepsilon_{\mathrm{sense}}$ and the aggregation energy, when n_{agg} raw streams are aggregated into a single stream, is $n_{\mathrm{agg}}\varepsilon_{\mathrm{agg}}$, which is also a constant term. Note that, in our proposed schemes, aggregation only takes place in the gateway (cluster head). However, because of the maximal ratio combining in the semirelay in the second cooperative scheme, we can approximate the MRC processing energy consumption in the semirelay with two-stream aggregation (two independent received signals being combined in the semirelay); in addition, in both the proposed cooperative schemes, the MRC processing consumption in the gateway is approximated with three-stream aggregation. Typical values for $\varepsilon_{\mathrm{agg}}$ and $\varepsilon_{\mathrm{sense}}$ are 5 and 50 nJ/bit, respectively [4], [31]. We use the following model for the energy dissipation per bit in the transmitter [4], [28], [31], [33]:

TABLE I
System Parameters

$f_c = 2.4GHz$	$\eta = .35$
$G_tG_r = 5dB$	$d_0 = 1m$
$N_o = -174\,dBm$	$M_l = 40\,dB$
$N_f = 10\,dB$	$P_e = 10^{-3}$
$r_s = 10\ ksps$	$N = 128$
$d_2 = 1\ m$	$d_6 = 1\ m$

$$\varepsilon_{\mathrm{Tx}}(d) = \frac{p_{\mathrm{tr}}^e}{br_s} + \varepsilon_{\mathrm{pl}} d^{\alpha} \quad (37)$$

where p_{tr}^e is a distance-independent term that takes into account the consumption power of the transmitter electronics (digital-to-analog converter, filters, mixer, and synthesizer). r_s is the symbol rate, b is the number of bits per symbol, and $\varepsilon_{\mathrm{pl}} d^{\alpha}$ (which accounts for the radiated power required to transmit one bit over a distance d between the source and the destination) depends on distance d, path loss exponent α, the acceptable bit error probability, the drain efficiency, and the amplifier peak-to-average power ratio (PAPR) [11], [28], [35]. The PAPR depends on the modulation scheme and the associated constellation size [35]. A typical value for the power consumption of the transmitter electronics is about $p_{\mathrm{tr}}^e = 96.3$ mW [11], [34], [35]. $\varepsilon_{\mathrm{pl}}$ can be calculated according to the link budget relationship [11], [28]

$$\varepsilon_{\mathrm{pl}} = \frac{\xi}{\eta} \varepsilon_b \left(\frac{4\pi d_0}{\lambda} \right)^2 \frac{M_l N_f}{G_t G_r} \left(\frac{1}{d_0} \right)^{\alpha} \quad (38)$$

where η is the drain efficiency, ξ is the PAPR, ε_b is the required average energy per bit for a given bit error probability, d_0 is the reference distance for the antenna far field, λ is the carrier wavelength, M_l is the link margin compensating the hardware variations, N_f is the receiver noise figure, G_t is the transmit antenna gain, G_r is the receive antenna gain, and α is the path loss exponent. In the proposed schemes, we have assumed that the path loss exponents in the Rayleigh links are equal to two, three, or four. However, in the Gaussian links, we can well assume that the path loss exponents for these links are two. In addition, the values of the PAPR (ξ) are equal to 1 and $3(\sqrt{M}-1)/(\sqrt{M}+1)$ for the BPSK and M-QAM modulations, respectively [35]. The system parameters used in our evaluations are based on [4], [11], [31], [34], and [35]. We have listed the other parameters in Table I. In the receiver, we assume that communication circuits expend energy $\varepsilon_{\mathrm{Rx}}$ to receive the message bit as follows [11], [35]:

$$\varepsilon_{\mathrm{Rx}} = \frac{p_{\mathrm{re}}^e}{br_s} \quad (39)$$

where b and r_s are defined in (37). A typical value for the receiver electronics power consumption is about $p^e_{\rm re} = 130.3$ mW [11], [34], [35].

In a general communication link connecting two wireless nodes, we can compute the total energy consumption for the transmission of one message bit, according to (37)–(39), as

$$\varepsilon_T = \frac{p^e_{\rm tr}}{br_s} + \frac{p^e_{\rm re}}{br_s} + \frac{\xi}{\eta}\varepsilon_b \left(\frac{4\pi d_0}{\lambda}\right)^2 \frac{M_l N_f}{G_t G_r}\left(\frac{d}{d_0}\right)^{\alpha}. \quad (40)$$

While the first and second terms in (40) are monotonically decreasing with b (the constellation size), the required average energy per bit, i.e., ε_b, in the third term is monotonically increasing with b. Thus, there exists an optimum value for b to minimize ε_T [11]. For the noncooperative and cooperative schemes one and two, the optimum constellation sizes of nodes S, P, and SR can be computed according to (40). Throughout this section, we assume that the transmitters (node S, P, or SR) send information symbols, with the optimum constellation sizes computed accordingly. We consider the system model of Section II for the noncooperative and cooperative schemes. As previously stated, in the noncooperative scheme, nodes S, P, and SR transmit their information symbols over the independent channels to the gateway. In addition, to maintain the same throughput as in the proposed cooperative schemes, nodes S and P transmit $N-1$ symbols for each block, and node SR, which is a type-A (low-load) node, transmits only two symbols during each block[6] [see Fig. 3(a)]. We first compute the total energy consumption of nodes S, P, and SR, and the gateway during a single block. In the noncooperative scheme, the total energy consumption in nodes S, P, and SR, and the gateway can be computed as follows:

$$\varepsilon^{\rm nc}_S = b_S\left((N-1)\varepsilon_{\rm sens} + (N-1)\frac{p^e_{\rm tr}}{b_S r_s} + (N-1)\varepsilon_{\rm pl} d_1^{\alpha}\right) \quad (41)$$

$$\varepsilon^{\rm nc}_P = b_P\left((N-1)\varepsilon_{\rm sens} + (N-1)\frac{p^e_{\rm tr}}{b_S r_s} + (N-1)\varepsilon_{\rm pl} d_4^{\alpha}\right) \quad (42)$$

$$\varepsilon^{\rm nc}_{\rm SR} = b_{\rm SR}\left(2\varepsilon_{\rm sens} + 2\frac{p^e_{\rm tr}}{b_{\rm SR} r_s} + 2\varepsilon_{\rm pl} d_6^{\alpha}\right) \quad (43)$$

$$\varepsilon^{\rm nc}_G = b_S(N-1)\frac{p^e_{\rm re}}{b_S r_s} + b_P(N-1)\frac{p^e_{\rm re}}{b_P r_s} + 2b_{\rm SR}\frac{p^e_{\rm re}}{b_{\rm SR} r_s} = 2N\frac{p^e_{\rm re}}{r_s} \quad (44)$$

where the d_i's are defined in Fig. 2(b), and b_S, b_P, and $b_{\rm SR}$ are the optimum constellation sizes in nodes S, P, and SR, respectively. Note that, in (44), the total energy consumption in the gateway does not depend on the constellation size. Moreover, because of the symmetry, the optimum constellation sizes of nodes S and P are equal, i.e., $b_S = b_P$.

Since the energy consumption of the data aggregation and the required energy to transmit the aggregated data to the sink (final destination) by the gateway node are similar in both the cooperative and noncooperative schemes, the aforementioned terms have no effect on the energy saving analysis, and we have omitted them in the energy consumption of the gateway given by (44). The average energy per bit required for computing $\varepsilon_{\rm pl}$ in (38) depends on the communication strategy (direct communication or cooperative communication), channel type (Gaussian or Rayleigh), and acceptable bit error probability P_b. In the noncooperative scheme (one path diversity), for Rayleigh channels, the average bit error probabilities of the BPSK and M-QAM modulations can be computed from (23) and (24), respectively, by setting $L = 1$. Note that, in (23) and (24), Λ is equal to (ε'/N_o). Therefore, by taking the inverse of the average bit error probability, we can obtain the required average energy per bit (i.e., $\varepsilon_b = \varepsilon'$) for a specified bit error probability value P_b. For Gaussian links, the average bit error probability of the BPSK and M-QAM modulations are given as [32]

$$P_e = Q\left(\sqrt{2\frac{\varepsilon}{N_o}}\right) \text{ for BPSK} \quad (45)$$

$$P_e \simeq \frac{4}{b}\left(\frac{\sqrt{M}-1}{\sqrt{M}}\right) Q\left(\sqrt{\frac{3b\varepsilon}{N_0(M-1)}}\right) \text{ for M-QAM} \quad (46)$$

respectively.

We can calculate the average energy consumption of the noncooperative system according to (41)–(44) as

$$\bar{\varepsilon}^{\rm nc}_{\rm total} = \frac{\varepsilon^{\rm nc}_S + \varepsilon^{\rm nc}_P + \varepsilon^{\rm nc}_{\rm SR} + \varepsilon^{\rm nc}_G}{(N-1)(b_S + b_p) + 2b_{\rm SR}}. \quad (47)$$

Now, we consider the proposed cooperative schemes. From the discussions of Sections III-A and B, we can use the bit error probabilities given by (23) and (24), with $L = 3$ and $L = 4$ as good approximations for the performance of schemes one and two, respectively. Unfortunately, it is difficult to find an explicit solution for Λ as a function of P_b; thus, we cannot find an explicit expression for ε or ε'. Therefore, we numerically compute Λ. The numerical solution gives $\varepsilon_b = \varepsilon'$, which is the required average bit energy for the given bit error probability; then, we can compute $\varepsilon_{\rm pl}$, which is given in (37), using (38). As stated in Section II-A, we have supposed that each transmission block with duration T contains $2N$ symbol intervals, and in cooperative scheme one, nodes S and P transmit $2N-2$ symbols and remain idle in the last two symbol intervals. In addition, node SR transmits its own two symbols and the $2N-2$ received symbols of nodes S and P ($N-1$ symbols for each node). Therefore, for cooperative

[6]The durations of information symbols in all of the nodes are $(T/N-1)$. Therefore, all of the nodes have similar symbol rates. However, node SR sends two symbols and remains idle in the remaining symbol intervals of the block (low-load node).

scheme one, the nodes' consumption energies are computed as follows:

$$\varepsilon_S^1 = b_S \left\{ (N-1)\varepsilon_{\text{sens}} + (2N-2)\frac{p_{\text{tr}}^e}{\left(\frac{2N}{N-1}\right) b_S r_s} + (2N-2)\varepsilon_{\text{pl}} d_1^\alpha + (N-1)\frac{p_{\text{re}}^e}{\left(\frac{2N}{N-1}\right) b_S r_s} \right\} \quad (48)$$

$$\varepsilon_P^1 = b_P \left\{ (N-1)\varepsilon_{\text{sens}} + (2N-2)\frac{p_{\text{tr}}^e}{\left(\frac{2N}{N-1}\right) b_P r_s} + (2N-2)\varepsilon_{\text{pl}} d_4^\alpha + (N-1)\frac{p_{\text{re}}^e}{\left(\frac{2N}{N-1}\right) b_P r_s} \right\} \quad (49)$$

$$\varepsilon_{\text{SR}}^1 = 2b_{\text{SR}} \left\{ \varepsilon_{\text{sens}} + \frac{p_{\text{tr}}^e}{\left(\frac{2N}{N-1}\right) b_{\text{SR}} r_s} + \varepsilon_{\text{pl}} d_6^\alpha \right\} + 2b_S \times (N-1) \left\{ \frac{p_{\text{tr}}^e}{\left(\frac{2N}{N-1}\right) b_S r_s} + \varepsilon_{\text{pl}} d_6^\alpha + b_S \frac{p_{\text{re}}^e}{\left(\frac{2N}{N-1}\right) b_S r_s} \right\} \quad (50)$$

$$\varepsilon_G^1 = \left(2(2N-2)+2N\right) \frac{p_{\text{re}}^e}{\left(\frac{2N}{N-1}\right) r_s} + 6\varepsilon_{\text{agg}}. \quad (51)$$

In the preceding derivation, we have utilized the fact that $b_S = b_P$. To maintain the same throughput as the noncooperative scheme, the source, partner, and semirelay in the cooperative schemes must increase the transmission symbol rates from r_s to $(2N/N-1)r_s$ (see Fig. 3). We have included this symbol rate increment in our energy consumption analysis. Moreover, like in (44) for the noncooperative scheme, the total energy consumption in (51) does not depend on the optimum constellation size. Finally, we can compute the average energy consumption of cooperative scheme one as follows:

$$\bar{\varepsilon}_{\text{total}}^1 = \frac{\varepsilon_S^1 + \varepsilon_P^1 + \varepsilon_{\text{SR}}^1 + \varepsilon_G^1}{(N-1)(b_S + b_p) + 2b_{\text{SR}}} \quad (52)$$

where ε_S^1, ε_P^1, $\varepsilon_{\text{SR}}^1$, and ε_G^1 are given in (48)–(51).

For scheme two, in the semirelay, we have $4\varepsilon_{\text{agg}}$ more energy consumption and $(2N-2)$ more symbol receptions than scheme one, and in this scheme, we must use (23) and (24) with $L=4$ for ε_b computation. Considering the preceding differences, we can easily obtain the average energy consumption of scheme two from (48)–(52).

V. Numerical Result and Comparison

In this section, we present some numerical results to illustrate the performance gains offered by the proposed protocols. For our evaluations, we have assumed $N=128$ and target rate $R=1$. In addition, Gaussian links are considered 6 dB stronger than Rayleigh uplinks, i.e., $\varepsilon = 4\varepsilon'$. First, we consider the diversity gains of our proposed schemes in Figs. 4–7. Fig. 4 shows the plots of P_{out}^1 versus Λ (Rayleigh uplink average received SNR) for the exact value of the outage probability computed from (16), the approximated value computed from (19), and the asymptotic value computed from (20). These result show that (18) is a good approximation for I_1 (the mutual information of scheme one) when ε is slightly greater (less than one order of magnitude) than ε'. For the sake of comparison, we have also plotted the noncooperative (direct transmission) outage probability [10]. As can be observed from Fig. 4, scheme one achieves a significant gain at the medium- to high-SNR regimes. For example, for an outage probability of 0.01, the SNR required by the noncooperative scheme is 20 dB, whereas, for scheme one, it is 8.37 dB. Fig. 5 compares the performance of the optimum detector given in (26) and the MRC detector for scheme two. The plots for the optimum detector are evaluated using Monte Carlo simulations, where BPSK modulation is considered. From Fig. 5, it can be observed that the MRC detector performs almost as well as the optimum detector given in (26) when the SNR in Gaussian channels is only slightly greater (less than one order of magnitude) than the SNR in Rayleigh fading channels.

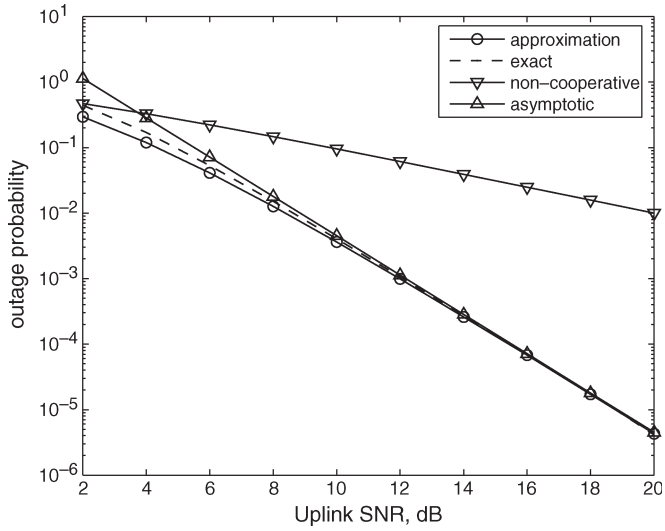

Fig. 4. Outage probability versus uplink SNR, where $N=128$, target rate $R=1$, and the Gaussian links are 6 dB stronger than the Rayleigh uplinks ($\varepsilon = 4\varepsilon'$).

Fig. 6 shows the plots of P_{out}^2 versus Λ for the outage probability based on the approximate mutual information given in (33) [which is derived by neglecting the noise term in (25)], the approximate value given in (35), and the asymptotic value given in (36). In addition, for the sake of comparison, we have plotted the outage probabilities for the noncooperative scheme and the proposed scheme one based on the mutual information given in (16). These results indicate the significant gain of scheme two against the noncooperative scheme and cooperative scheme one. For instance, for the outage probability of 0.01, the required SNRs in the noncooperative scheme and cooperative scheme one are 20 and 8.5 dB, respectively,

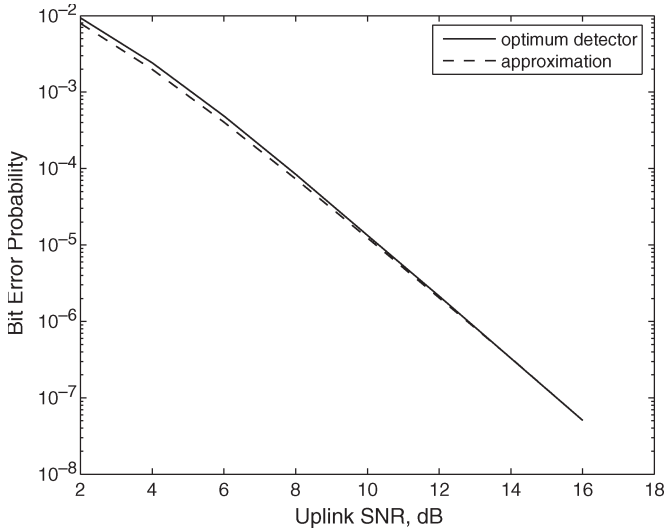

Fig. 5. Bit error probability versus uplink SNR. Gaussian links are 6 dB stronger than Rayleigh uplinks ($\varepsilon = 4\varepsilon'$).

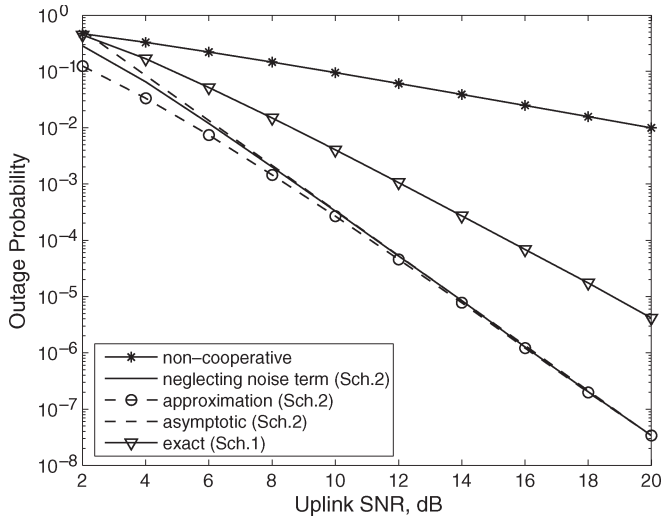

Fig. 6. Outage probability versus uplink SNR, where $N = 128$, target rate $R = 1$, and the Gaussian links are 6 dB stronger than the Rayleigh uplinks ($\varepsilon = 4\varepsilon'$).

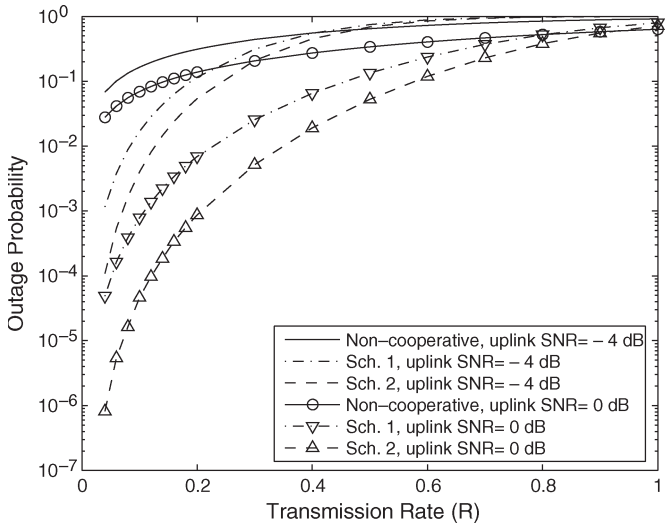

Fig. 7. Outage probability versus transmission rate R, where $N = 128$, and the Gaussian links are 6 dB stronger than the Rayleigh uplinks ($\varepsilon = 4\varepsilon'$).

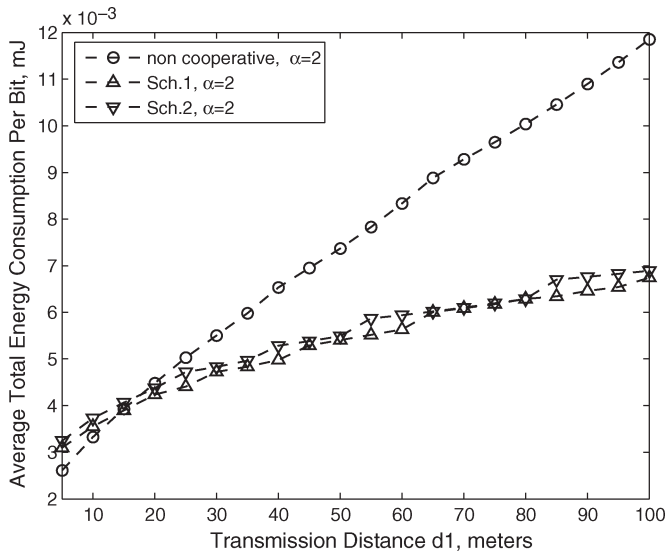

Fig. 8. Average total energy consumption per bit versus the source distance from the gateway. The path loss exponent is equal to 2.

whereas, for cooperative scheme two, the required SNR is 6.13 dB. To investigate the performance of the proposed cooperative schemes for a fixed SNR at the variable-rate regimes, in Fig. 7, we have plotted the outage probability versus rate R for both the cooperative and noncooperative schemes for various values of the uplink SNR Λ. We observe that, at very low Λ, e.g., -4 dB, the outage probabilities of the cooperative schemes are greater than those of the noncooperative scheme at high-rate regimes. However, at the higher values of Λ, e.g., 0 dB, the outage probabilities of the cooperative schemes are smaller than the outage probability of the noncooperative scheme for almost all of the rates considered. Moreover, these results show that the cooperative schemes always perform better than the noncooperative scheme at low-rate regimes.

Now, we present some numerical results to compare the energy efficiencies of schemes one and two with the noncooperative scheme and the CST scheme proposed in [11]. To investigate the effect of path loss exponent α, we have computed the optimized average energy consumption of the noncooperative and cooperative schemes for various values of α. Figs. 8 and 9 show the plots of the average energy consumption per bit versus transmission distance d_1 for various path loss exponents α. In all of the evaluations, we have used the system parameters given in Table I. From Fig. 8 ($\alpha = 2$), significant energy can be saved by the node cooperation under the same throughput and bit error probability constraints. For example, schemes one and two offer about a 75% energy saving compared to the noncooperative scheme for $d_1 = 100$ m. As we can see from Fig. 8, for all of the distances less than 100 m, schemes one and two have almost the same energy efficiencies. Now, we compare our proposed schemes with the CST scheme proposed in [11]. The results in [11] indicate that the critical distance

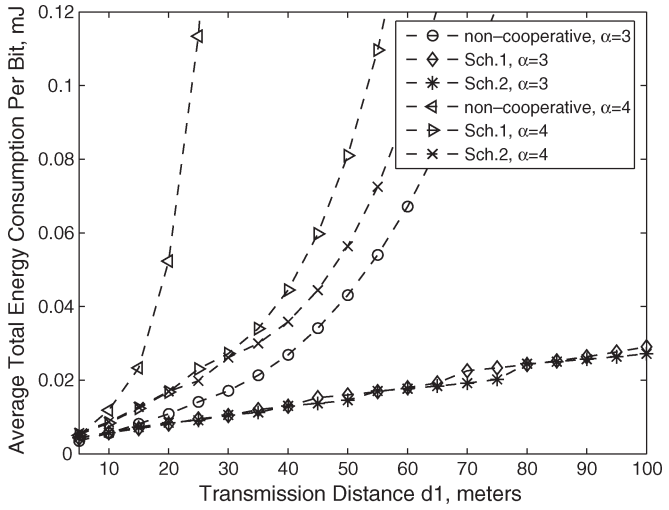

Fig. 9. Average total energy consumption per bit versus the source distance from the gateway. The path loss exponent is equal to 3 and 4.

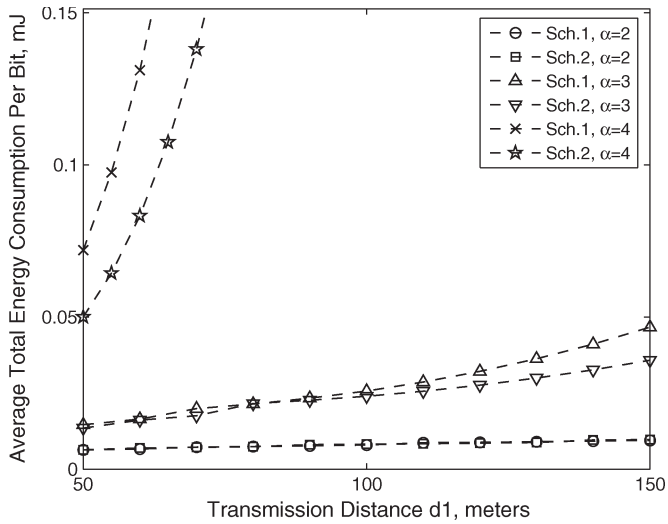

Fig. 10. Average energy consumption of the cooperative schemes one and two per bit versus the source distance from the gateway. We have used the parameters' values given in Table I.

below which the noncooperative system beats the CST scheme of [11] in terms of the energy efficiency is about 27.5 m, and this scheme offers a 100% energy saving for $d_1 = 100$ m. However, for our proposed schemes, simulation results in Fig. 8 show that the critical distance is about 20 m, and about 75% energy saving is achieved for the same distance of 100 m. Although the CST scheme has 25% more energy saving in comparison with our proposed schemes, take note that Cui *et al.* [11] have considered an error-free link between the nodes and their partners. In fact, for the energy consumption analysis, they did not take into account the error propagation in the space-time code transmission. In fact, if we consider the effect of error propagation, for instance, in a 2×1 multiple-input–single-output system based on Alamouti space-time code with BPSK modulation, our further simulation results show that the source node in the scheme [11] must increase its transmission energy by about 1.7 dB to achieve the same final bit error probability of 0.001 as in [11]. In this simulation, we have assumed that the link between the source and its partner has bit error probability $P_e = 10^{-3}$. Certainly, if we also consider the error propagation effect in the receiver side (link between node SR and the gateway), the total penalty for the CST scheme will be increased by much more than 1.7 dB.

Fig. 9 shows the average energy consumption versus transmission distance d_1 for path loss exponents of three and four. From Fig. 9, a remarkable amount of energy can be saved by the node cooperation in highly scattered environments. For instance, more than 200% energy can be saved, even at a short transmission distance $d_1 = 20$ m for $\alpha = 4$. An important observation from Figs. 8 and 9 is that, as α increases, schemes one and two are more energy efficient than the noncooperative scheme, even for very short transmission distances.

To compare the performance between schemes one and two, we consider various path loss exponents. Fig. 10 compares the performance of the proposed schemes one and two. From Fig. 10, we observe that, for an ideal propagation channel in which $\alpha = 2$, schemes one and two have the same energy efficiency. However, for highly scattered environments (for instance, $\alpha = 3$ and $\alpha = 4$), there exists a threshold distance (about 85 m for $\alpha = 3$ and about 20 m for $\alpha = 4$) above which scheme two becomes more energy efficient than scheme one. In addition, Fig. 10 shows that scheme two achieves significant energy saving in the highly scattered environments. For example, about a 60% energy saving is achieved compared to scheme one for a distance of $d_1 = 60$ m in the environment with a path loss exponent of $\alpha = 4$.

VI. Conclusion

This paper has presented two cooperative schemes for heterogeneous wireless sensor networks that use the AF cooperative strategy in the transmitters and maximal ratio combining in the receivers. The outage probability and the bit error probability of the proposed schemes for the BPSK and M-QAM modulations have been evaluated. Analytical results have indicated that the proposed schemes one and two achieve the diversity orders of three and four, respectively. In addition, the total energy consumption analysis has shown that the performance enhancement provided by the cooperative scheme leads to the energy consumption saving for the same reliability compared to the noncooperative scheme.

Even though the complicated cooperative scheme two achieves higher order diversity than the relatively simple scheme one, the evaluations have shown that this higher order diversity cannot properly compensate for the computational complexity of scheme two in the ideal channel propagation (free space with path loss exponent two). However, our results have indicated that scheme two achieves significant energy saving in highly scattered environments compared to scheme one. We observe that, in the highly scattered environments, our proposed schemes can save more energy, even in short- (few tens of meters) to medium-range (several tens of meters) distances, in comparison with the noncooperative scheme.

APPENDIX A
MUTUAL INFORMATION OF SCHEME ONE

In this Appendix, we derive (16). First, we rewrite (3)–(5) into vector form as

$$\underbrace{\begin{bmatrix} y_{G,S}[i] \\ y_{G,P}[i+1] \\ y_{G,\mathrm{SR}}[i+2] \end{bmatrix}}_{\mathbf{y}_1} = \underbrace{\begin{bmatrix} \sqrt{\varepsilon'}a_{G,S} \\ \beta\sqrt{\varepsilon}a_{G,P} \\ \beta'\sqrt{\varepsilon'}a_{\mathrm{SR},S} \end{bmatrix}}_{A_1} x_S[i] + \underbrace{\begin{bmatrix} 1 & 0 & 0 & 0 & 0 \\ 0 & \beta a_{G,P} & 0 & 1 & 0 \\ 0 & 0 & \beta' & 0 & 1 \end{bmatrix}}_{B_1} \underbrace{\begin{bmatrix} z_{G,S}[i] \\ z_{P,S}[i] \\ z_{\mathrm{SR},S}[i] \\ z_{G,P}[i+1] \\ z_{G,\mathrm{SR}}[i+2] \end{bmatrix}}_{n_1} \quad (53)$$

where β and β' are given in (7), and for the source signal, we have

$$E\left\{|x_S[i]|^2\right\} = 1. \quad (54)$$

From the vector results in [33], the maximum average mutual information, which is achieved with an i.i.d. zero-mean circular symmetric complex Gaussian source signal, is

$$I(x_S, y_1) = \frac{N-1}{2N}\log_2 \det \times \left(1_{3\times 3} + \left(A_1 A_1^H\right)\left(B_1 E\left\{n_1 n_1^H\right\} B_1^H\right)^{-1}\right) \quad (55)$$

where H and $1_{3\times 3}$ denote the Hermitian and a 3×3 identity matrix, respectively. Note that the factor $N - 1/(2N)$ in (55) is due to the fact that, for every $N-1$ transmission symbol in the noncooperative scheme, each node S and P must transmit $2N$ symbols in the cooperative schemes. With some algebraic simplifications, we have the equations shown at the bottom of the page. Thus, we have

$$I(x_S, y_1) = \frac{N-1}{2N} \times \log_2\left(1 + \frac{\varepsilon'|a_{G,S}|^2}{N_o} + \frac{\beta^2\varepsilon|a_{G,P}|^2}{N_o + N_o\beta^2|a_{G,P}|^2} + \frac{\beta'^2\varepsilon'|a_{\mathrm{SR},S}|^2}{N_o + N_o\beta'^2}\right). \quad (56)$$

Now, by substituting the values of β and β' from (7) in (56), we easily obtain

$$I_1 = \frac{N-1}{2N} \times \log_2\left(1 + \eta_{G,S} + \frac{\eta_{P,S}\eta_{G,P}}{\eta_{P,S} + \eta_{G,P} + 1} + \frac{\eta_{\mathrm{SR},S}\eta_{G,\mathrm{SR}}}{\eta_{\mathrm{SR},S} + \eta_{G,\mathrm{SR}} + 1}\right) \quad (57)$$

where the $\eta_{i,j}$'s, i.e., the instantaneous received SNR, are given in (15).

APPENDIX B
OUTAGE PROBABILITY OF SCHEME ONE

The proof of (19) is presented in this Appendix. We know that

$$P_{\mathrm{out}}^1 \simeq \Pr\{I_1 < R\} = \Pr\left\{\eta_{G,S} + \eta_{G,P} + \eta_{\mathrm{SR},S} < 2^{\left(\frac{2N}{N-1}\right)R} - 1\right\}. \quad (58)$$

Since the $\eta_{i,j}$'s are independent exponential distributed random variables, their summation in (58) follows a chi-square distribution with a degree of freedom equal to six. Therefore, we have

$$\begin{aligned} P_{\mathrm{out}}^1 &\simeq \int_0^{2^{\left(\frac{2N}{N-1}\right)R}-1} \frac{x^2}{2\Lambda^3} e^{-\frac{x}{\Lambda}} dx \\ &= \gamma_{\mathrm{inc}}\left(3, \frac{2^{\left(\frac{2N}{N-1}\right)R} - 1}{\Lambda}\right) \\ &= 1 - e^{-\frac{2^{\left(\frac{2N}{N-1}\right)R}-1}{\Lambda}} \left(\sum_{m=0}^{2} \frac{\left(\frac{2^{\frac{2N}{N-1}R}-1}{\Lambda}\right)^m}{m!}\right) \end{aligned} \quad (59)$$

where Λ is given in (17). To derive the asymptotic behavior, we define $\rho = (2^{(2N/N-1)R} - 1/\Lambda)$, and we compute the following limit:

$$\lim_{\Lambda\to\infty} \frac{P_{\mathrm{out}}^1}{(1/\Lambda)^3} = \lim_{\rho\to 0} \frac{1 - e^{-\rho}\left(\sum_{m=0}^{2} \frac{\rho^m}{m!}\right)}{\left(2^{\left(\frac{2N}{N-1}\right)R} - 1\right)^{-3}\rho^3} = \frac{1/6}{\left(2^{\left(\frac{2N}{N-1}\right)R} - 1\right)^{-3}}.$$

As a result, we easily derive (20).

$$A_1 A_1^H = \begin{bmatrix} \varepsilon'|a_{G,S}|^2 & \beta\sqrt{\varepsilon\varepsilon'}a_{G,S}a_{G,P}^* & \beta'\varepsilon' a_{G,S}a_{\mathrm{SR},S}^* \\ \beta\sqrt{\varepsilon\varepsilon'}a_{G,S}^* a_{G,P} & \beta^2\varepsilon|a_{G,P}|^2 & \beta\beta'\sqrt{\varepsilon\varepsilon'}a_{\mathrm{SR},S}^* a_{G,P} \\ \beta'\varepsilon' a_{G,S}^* a_{\mathrm{SR},S} & \beta\beta'\sqrt{\varepsilon\varepsilon'}a_{\mathrm{SR},S}a_{G,P}^* & \beta'^2\varepsilon'|a_{\mathrm{SR},S}|^2 \end{bmatrix}$$

$$B_1 E\left\{n_1 n_1^H\right\} B_1^H = N_o \begin{bmatrix} 1 & 0 & 0 \\ 0 & 1+\beta^2|a_{G,P}|^2 & 0 \\ 0 & 0 & 1+\beta'^2 \end{bmatrix}$$

APPENDIX C
OPTIMUM DETECTOR AND THE MUTUAL INFORMATION OF SCHEME TWO

Optimal Detector

First, by substituting (1) and (10), we expand (8) and (11). After some algebraic simplifications, we write (3), (8), and (11) in the following vector form:

$$\underbrace{\begin{bmatrix} y_{G,S} \\ y_{G,P} \\ y_{G,\mathrm{SR}} \end{bmatrix}}_{y_2} = \underbrace{\begin{bmatrix} \sqrt{\varepsilon'}a_{G,S} \\ \beta\sqrt{\varepsilon}a_{G,P} \\ \beta''\mathrm{SNR}_{\mathrm{SR}} \end{bmatrix}}_{A_2} x_S + B_2 \times \underbrace{\begin{bmatrix} z_{G,S} \\ z_{P,G} \\ z_{\mathrm{SR},S} \\ z_{G,P} \\ z_{\mathrm{SR},P} \\ z_{G,\mathrm{SR}} \end{bmatrix}}_{n_2} \tag{60}$$

where B_2 is given by (61), shown at the bottom of the page. Note that, in (60), we have omitted the slot indexes for simplification. Now, we assume a system with BPSK modulation and coherent receiver in the gateway. In this case, all of the noise terms in the receivers, i.e., the elements of vector n_2, are replaced by independent real zero-mean white Gaussian noise $n_{i,j}$ with variance $\sigma^2 = (N_o/2)$, and all of the complex circular symmetric Gaussian fading coefficients, i.e., $a_{i,j}$'s, are replaced with Rayleigh distributed coefficients $|a_{i,j}|$. Therefore, we can rewrite (60) and (61) as follows:

$$\underbrace{\begin{bmatrix} y_{G,S} \\ y_{G,P} \\ y_{G,\mathrm{SR}} \end{bmatrix}}_{y_2} = \underbrace{\begin{bmatrix} \sqrt{\varepsilon'}|a_{G,S}| \\ \beta\sqrt{\varepsilon}|a_{G,P}| \\ \beta''\mathrm{SNR}_{\mathrm{SR}} \end{bmatrix}}_{A_2} x_S + B_2 \times \underbrace{\begin{bmatrix} n_{G,S} \\ n_{P,S} \\ n_{\mathrm{SR},S} \\ n_{G,P} \\ n_{\mathrm{SR},P} \\ n_{G,\mathrm{SR}} \end{bmatrix}}_{n_2} \tag{62}$$

where B_2 is given by (63), shown at the bottom of the page. The optimal detector of x_S based on the received vector y_2 is the maximum *a posteriori* probability detector, i.e., the optimal detector has the following decision rule:

$$\begin{aligned} \hat{x}_S &= \arg\max_{x_S} f_{x_S|y_2}(y_2) \\ &= \arg\max_{x_S} f_{y_2|x_S}(y_2)\frac{P_{x_S}}{f_{y_2}(y_2)} \\ &= \arg\max_{x_S} f_{y_2|x_S}(y_2) \end{aligned} \tag{64}$$

where the third equality results from the assumption of equiprobable bits. Conditioned on $n_{P,S}$, i.e., the noise term in the link between the source and the partner, and the fading coefficients, the elements of the vector y_2 are independent Gaussian random variables. Thus, we have

$$\begin{aligned} f(y_2|x_S, n_{P,S}) &= f(y_{G,S}|x_S, n_{P,S}) \\ &\quad \times f(y_{G,P}|x_S, n_{P,S}) \times f(y_{G,\mathrm{SR}}|x_S, n_{P,S}). \end{aligned} \tag{65}$$

Then

$$\begin{aligned} f(y_2|x_S) = \frac{1}{\sqrt{2\pi\sigma^2}} \int_{-\infty}^{+\infty} & f(y_{G,S}|x_S, n_{P,S}) f(y_{G,P}|x_S, n_{P,S}) \\ & \times f(y_{G,\mathrm{SR}}|x_S, n_{P,S}) e^{-\frac{n_{P,S}^2}{2\sigma^2}} dn_{P,S}. \end{aligned} \tag{66}$$

Now, if we substitute the corresponding Gaussian probability density functions in (66), after some straightforward simplifications, we obtain

$$f(y_2|x_S) = K \exp\left(Dy_1^2 + Ey_2^2 + Fy_3^2 + Hy_2y_3\right) \tag{67}$$

where y_1, y_2, and y_3 are defined as follows:

$$y_1 = y_{G,S} - \sqrt{\varepsilon'}|a_{G,S}|x_S \triangleq y_{G,S} - b_1 x_S \tag{68}$$

$$y_2 = y_{G,P} - \beta\sqrt{\varepsilon}|a_{G,P}|x_S \triangleq y_{G,P} - b_2 x_S \tag{69}$$

$$y_3 = y_{G,\mathrm{SR}} - \beta''\mathrm{SNR}_{\mathrm{SR}} x_S \triangleq y_{G,\mathrm{SR}} - b_3 x_S \tag{70}$$

and constants D, E, F, H, and K are given by

$$\begin{aligned} D &= -\frac{1}{2\sigma^2} \\ E &= \frac{k_2^2}{4a\sigma^4} - \frac{1}{2\sigma^2} \\ F &= \frac{k_2'^2}{4a\sigma^4\left(k_3^2 + k_5^2 + 1\right)^2} - \frac{1}{2\sigma^2\left(k_3^2 + k_5^2 + 1\right)} \\ H &= \frac{k_2 k_2'}{2a\sigma^4\left(k_3^2 + k_5^2 + 1\right)} \\ K &= \sqrt{\frac{\pi}{a}}\frac{1}{2\pi^2\sigma^4\sqrt{k_3^2 + k_5^2 + 1}} \end{aligned} \tag{71}$$

$$B_2 = \begin{bmatrix} 1 & 0 & 0 & 0 & 0 & 0 \\ 0 & \beta a_{G,P} & 0 & 1 & 0 & 0 \\ 0 & \frac{\beta^2\beta''\sqrt{\varepsilon}|a_{\mathrm{SR},P}|^2}{\beta^2|a_{\mathrm{SR},P}|^2 N_o + N_o} & \frac{\beta''\sqrt{\varepsilon'}a_{\mathrm{SR},S}^*}{N_o} & 0 & \frac{\beta\beta''\sqrt{\varepsilon}a_{\mathrm{SR},P}^*}{\beta^2|a_{\mathrm{SR},P}|^2 N_o + N_o} & 1 \end{bmatrix} \tag{61}$$

$$B_2 = \begin{bmatrix} 1 & 0 & 0 & 0 & 0 & 0 \\ 0 & \beta|a_{G,P}| & 0 & 1 & 0 & 0 \\ 0 & \frac{\beta^2\beta''\sqrt{\varepsilon}|a_{\mathrm{SR},P}|^2}{\beta^2|a_{\mathrm{SR},P}|^2 N_o + N_o} & \frac{\beta''\sqrt{\varepsilon}|a_{\mathrm{SR},S}|}{N_o} & 0 & \frac{\beta\beta''\sqrt{\varepsilon}|a_{\mathrm{SR},P}|}{\beta^2|a_{\mathrm{SR},P}|^2 N_o + N_o} & 1 \end{bmatrix} \triangleq \begin{bmatrix} 1 & 0 & 0 & 0 & 0 & 0 \\ 0 & k_2 & 0 & 1 & 0 & 0 \\ 0 & k_2' & k_3 & 0 & k_5 & 1 \end{bmatrix} \tag{63}$$

where k_2, k_2', k_3, and k_5 are defined in (63), and the parameter "a" in (71) is defined as follows:

$$a = \frac{k_2^2}{2\sigma^2} + \frac{k_2'^2}{2\sigma^2\left(k_3^2 + k_5^2 + 1\right)} + \frac{1}{2\sigma^2}.$$

According to (64), the decision rule for the optimal detector is given by

$$f(y_2|x_S = 1) \underset{-1}{\overset{+1}{\gtrless}} f(y_2|x_S = -1). \tag{72}$$

By substituting (67) in (72), the optimum detector given in (26) is derived.

Mutual Information

Now, we derive the mutual information between the source and the gateway. By neglecting the noise term $z_{P,S}[i]$ in (25), the derivation of the approximated mutual information for scheme two is similar to that of scheme one. By substituting (60) in the mutual information formula given in (55), we derive the approximated mutual information $I(x_S, y_2)$ as follows:

$$I(x_S, y_2) \simeq \frac{N-1}{2N} \times \log_2 \det \left(1_{3\times 3} + \left(A_2 A_2^H\right) \times \left(B_2' E\left\{n_2 n_2^H\right\} {B_2'}^H\right)^{-1} \right) \tag{73}$$

where y_2, A_2, and n_2 are defined in (60), and B_2' is equal to B_2 in (61), except that the component $B_2'(3, 2)$ of this matrix is replaced with zero because we neglect the noise term in (25). Substituting these matrix values into (73) and after some straightforward simplifications, we obtain

$$I(x_S, y_2) \simeq \frac{N-1}{2N} \log_2 \left(1 + snr_1 + snr_2 + snr_3\right) \tag{74}$$

where the snr_i's are defined in (29).

ACKNOWLEDGMENT

The authors would like to thank Prof. M. Valenti and the anonymous reviewers for their helpful comments and suggestions, which considerably improved this paper.

REFERENCES

[1] I. F. Akyildiz, W. Su, Y. Sankarasubramaniam, and E. Cayirci, "Wireless sensor networks: A survey," *Comput. Netw.*, vol. 38, no. 4, pp. 393–422, Mar. 2002.

[2] "Exploratory research: Heterogeneous sensor networks," *Intel Technology Journal: Research and Development at Intel*, 2004. [Online]. Available: http://www.intel.com/research/exploratory/heterogeneous.htm

[3] V. Mhatre, C. Rosenberg, D. Kofman, R. Mazumdar, and N. Shroff, "A minimum cost heterogeneous sensor network with a lifetime constraint," *IEEE Trans. Mobile Comput.*, vol. 4, no. 1, pp. 4–15, Jan./Feb. 2005.

[4] W. Heinzelman, A. P. Chandrakasan, and H. Balakrishnan, "An application-specific protocol architecture for wireless microsensor networks," *IEEE Trans. Wireless Commun.*, vol. 1, no. 4, pp. 660–670, Oct. 2002.

[5] R. Ramanathan and R. Hain, "Topology control of multihop wireless radio networks using transmit power adjustment," in *Proc. IEEE INFOCOM*, Tel Aviv, Israel, Mar. 2000, pp. 404–413.

[6] W. Ye, J. Heidemann, and D. Estrin, "An energy-efficient MAC protocol for wireless sensor networks," in *Proc. 21st INFOCOM*, New York, Jun. 2002, pp. 1567–1576.

[7] A. Cerpa and D. Estrin, "ASCENT: Adaptive self-configuring sensor networks topologies," in *Proc. 21st Int. Annu. Joint Conf. IEEE Comput. Commun. Soc.*, New York, Jun. 23–27, 2002, pp. 1278–1287.

[8] Y. Yu, R. Govindan, and D. Estrin, "Geographical and energy aware routing: A recursive data dissemination protocol for wireless sensor networks," Comput. Sci. Dept., Univ. Calif., Los Angeles, CA, Tech. Rep. UCLA/CSD-TR-01-0023, May 2001.

[9] I. Chatzigiannakis, A. Kinalis, and S. Nikoletseas, "An adaptive power conservation scheme for heterogeneous wireless sensor networks with node redeployment," in *Proc. 17th Annu. SPAA*, 2005, pp. 96–105.

[10] J. N. Laneman, D. N. C. Tse, and G. W. Wornell, "Cooperative diversity in wireless networks: Efficient protocols and outage behavior," *IEEE Trans. Inf. Theory*, vol. 50, no. 12, pp. 3062–3080, Dec. 2004.

[11] S. Cui, A. J. Goldsmith, and A. Bahai, "Energy-efficiency of MIMO and cooperative MIMO techniques in sensor networks," *IEEE J. Sel. Areas Commun.*, vol. 22, no. 6, pp. 1089–1098, Aug. 2004.

[12] N. Jindal, U. Mitra, and A. J. Goldsmith, "Capacity of ad-hoc networks with node cooperation," in *Proc. IEEE Int. Symp. Inf. Theory*, 2004, p. 271. Also in preparation for *IEEE Trans. Inf. Theory*.

[13] J. M. Shea, T. F. Wong, and W.-H. Wong, "Cooperative-diversity slotted ALOHA," in *Proc. ACM/Wireless Networks QShine—Special Issue*, 2005, p. 35.

[14] S. K. Jayaweera, "Virtual MIMO-based cooperative communication for energy-constrained wireless sensor networks," *IEEE Trans. Wireless Commun.*, vol. 5, no. 5, pp. 984–989, May 2006.

[15] A. Wittneben, "Coherent multiuser relaying with partial relay cooperation," in *Proc. IEEE WCNC*, Apr. 3–6, 2006, pp. 1027–1033.

[16] P. Liu, Z. Tao, S. Narayanan, T. Korakis, and S. Panwar, "CoopMAC: A cooperative MAC for wireless LANs," *IEEE J. Sel. Areas Commun.—Special Issue Cooperative Communications Networking*, vol. 25, no. 2, pp. 340–354, Feb. 2007.

[17] M. Kuhn, S. Berger, I. Hammerstrom, and A. Wittneben, "Power line enhanced cooperative wireless communications," *IEEE J. Sel. Areas Commun.*, vol. 24, no. 7, pp. 1401–1410, Jul. 2006.

[18] B. Zhao and M. C. Valenti, "Practical relay networks: A generalization of hybrid-ARQ," *IEEE J. Sel. Areas Commun.*, vol. 23, no. 1, pp. 7–18, Jan. 2005.

[19] G. Kramer, M. Gastpar, and P. Gupta, "Cooperative strategies and capacity theorems for relay networks," *IEEE Trans. Inf. Theory*, vol. 51, no. 9, pp. 3037–3063, Feb. 2004.

[20] A. Sendonaris, E. Erkip, and B. Aazhang, "User cooperation diversity—Part I: System description," *IEEE Trans. Commun.*, vol. 51, no. 11, pp. 1927–1938, Nov. 2003.

[21] A. Sendonaris, E. Erkip, and B. Aazhang, "User cooperation diversity—Part II: Implementation, aspects and performance analysis," *IEEE Trans. Commun.*, vol. 51, no. 11, pp. 1939–1948, Nov. 2003.

[22] A. Wittneben, I. Hammerstroem, and M. Kuhn, "Joint cooperative diversity and scheduling in low mobility wireless networks," in *Proc. GLOBECOM*, Dallas, TX, Nov. 29–Dec. 3, 2004, pp. 780–784.

[23] J. Nicholas Laneman and G. W. Wornell, "Distributed space-time coded protocols for exploiting cooperative diversity in wireless networks," *IEEE Trans. Inf. Theory*, vol. 49, no. 10, pp. 2415–2425, Oct. 2003.

[24] T. E. Hunter and A. Nosratinia, "Diversity through coded cooperation," *IEEE Trans. Wireless Commun.*, vol. 5, no. 2, pp. 283–289, Feb. 2006.

[25] B. Zhao and M. C. Valenti, "Distributed turbo coded diversity for the relay channel," *Electron. Lett.*, vol. 39, no. 10, pp. 786–787, May 2003.

[26] A. Stefanov and E. Erkip, "Cooperative coding for wireless networks," *IEEE Trans. Commun.*, vol. 52, no. 9, pp. 1470–1476, Sep. 2004.

[27] S. M. Alamouti, "A simple transmit diversity technique for wireless communications," *IEEE J. Sel. Areas Commun.*, vol. 16, no. 8, pp. 1451–1458, Oct. 1998.

[28] J. G. Proakis, *Digital Communications*, 4th ed. New York: McGraw-Hill, 2001.

[29] E. Telator, "Capacity of multi-antenna Gaussian channels," *Eur. Trans. Telecommun.*, vol. 10, no. 6, pp. 585–596, Nov./Dec. 1999.

[30] I. S. Gradshteyn and I. M. Ryzhink, *Table of Integrals Series and Products*. New York: Academic, 1965.

[31] M. Bhardwaj and A. Chandrakasan, "Bounding the lifetime of sensor networks via optimal role assignments," in *Proc. IEEE INFOCOM*, 2002, pp. 1587–1596.

[32] M. K. Simon and M.-S. Alouini, *Digital Communication over Fading Channels: A Unified Approach to Performance Analysis*, 2nd ed. Hoboken, NJ: Wiley, 2005.

[33] X. Li, M. Chen, and W. Liu, "Application of STBC-encoded cooperative transmissions in wireless sensor networks," *IEEE Signal Process. Lett.*, vol. 12, no. 2, pp. 134–137, Feb. 2005.
[34] E. Shih *et al.*, "Physical layer driven protocol and algorithm design for energy-efficient wireless sensor networks," in *Proc. ACM Mobicom*, Jul. 20, 2001, pp. 272–287.
[35] S. Cui, A. J. Goldsmith, and A. Bahai, "Energy-constrained modulation optimization," *IEEE Trans. Wireless Commun.*, vol. 4, no. 5, pp. 2349–2360, Sep. 2005.

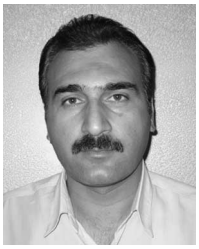

Azizollah Jamshidi (S'06) received the B.S. degree (with honors) from Shiraz University, Shiraz, Iran, in 1997 and the M.S. degree from Sharif University of Technology, Tehran, Iran, in 1999, both in electrical engineering. He is currently working toward the Ph.D. degree in electrical engineering with the Sharif University of Technology.

Since February 2003, he has been a member of the Wireless Research Laboratory, Department of Electrical Engineering, Sharif University of Technology. His current research interests include cooperative networks, cognitive radios, channel coding, and information theory.

Masoumeh Nasiri-Kenari (S'90–M'94) received the B.S. and M.S. degrees from Isfahan University of Technology, Isfahan, Iran, in 1986 and 1987, respectively, and the Ph.D. degree from the University of Utah, Salt Lake City, in 1993, all in electrical engineering.

From 1987 to 1988, she was a Technical Instructor and Research Assistant with Isfahan University of Technology. Since 1994, she has been with the Department of Electrical Engineering, Sharif University of Technology, Tehran, Iran, where she is currently a Professor and the Director of the Wireless Research Laboratory. From 1999 to 2001, she was a Codirector of the Advanced Communication Science Research Laboratory, Iran Telecommunication Research Center, Tehran. Her current research interests are wireless communication systems, error-correcting codes, and optical communication systems.